First- and second-order transitions for a superconducting cylinder in a magnetic field obtained from a self-consistent solution of the Ginzburg-Landau equations

G. F. Zharkov

P.N. Lebedev Physics Institute, Russian Academy of Sciences, Moscow, 117924, Russia

Based on self-consistent solution of nonlinear GL equations, the phase boundary is found, which divides the regions of first- and second-order phase transitions to normal state of a superconducting cylinder of radius R, placed in magnetic field and remaining in the state of fixed vorticity m. This boundary is a complicated function of the parameters (m,R,κ) (κ is the GL parameter), which does not coincide with the simple phase boundary $\kappa = 1/\sqrt{2}$, dividing the regions of first- and second-order phase transitions in infinite (open) superconducting systems.

I. INTRODUCTION

The GL theory is widely used for studying the general properties of the superconducting state. This theory leads to two coupled three-dimensional nonlinear equations for the order parameter ψ and magnetic field vector potential $\mathbf{A}$, which are usually solved using various simplifying assumptions. The self-consistent solutions of GL equations in the particular case of a long superconducting cylinder of radius R, placed in the axial magnetic field H, were found first by Fink *et al.*[1,2] In this case the three-dimensional GL equations reduce to the one-dimensional form, what simplifies the calculations and enables one to study the specific nonlinear effects, as well as the role of the sample boundary. Later, the one-dimensional equations were also addressed in Refs. 3–8. (Strictly speaking, in Refs. 4,5 the case of thin superconducting disk in a perpendicular magnetic field was considered, which models the geometry, used in experiments.[9] The physics of the processes in disks[4,5,9] and cylinders[2,3,6–8] may differ, however, many qualitative results are similar for different geometries.) As was shown in Refs. 6,7 the one-dimensional solution for the order parameter ψ (with fixed vorticity m) may change its form (under the influence of the external field H) either gradually [in one interval of the parameters (R,κ), κ is the GL parameter], vanishing by the second-order phase transition, or abruptly [in the other interval of (R,κ)], undergoing the first-order jump transformation. Such jump transformations, in principle, may be observable, because they are accompanied by jumps of the magnetization $M(H)$. It is shown below, that these jumps, and also the presence (or absence) of the tails in the magnetization curves, play important roles, enabling one to find the boundary between the first and second-order phase transitions in superconducting cylinder.

[The jump transformations of the self-consistent solutions of GL equations were encountered first by Fink and Presson.[2] However, they did not pay much attention to the ''tails,'' which remain in the magnetization curves after the points of a jump (see, for details, Figs. 1–5 below), and disregarded them completely, as being not characteristic for the superconducting state (see a footnote in Ref. 2a, p. 400). The jumps in the magnetization for disks are present also in some of the curves, found numerically by Schweigert and Peeters (see Figs. 19 and 20 in Ref. 4c). (The one-dimensional solutions for a long cylinder were studied also in Ref. 3, but, unfortunately, most of the numerical results, presented there, contain errors.) The physics behind the jump transitions within the states of fixed m, and between the states of different vorticities, is different. Probably, in the experiments with mesoscopic disks[9] both types of transitions may be seen. However, the connection with experiment will not be discussed here in detail (partly, because the long-cylinder models the thin-disk geometry rather poorly). We will concentrate below on the investigation of some formal properties of the solutions, what may give the additional insight into the complicated picture, observed experimentally.]

In the present paper the phase boundary is found, which divides the region of parameters (R,κ), where the superconducting solution of fixed m terminates (in the increasing external field) by the first-order jump to normal state ($\psi \equiv 0$), from the region (R,κ), where the solution vanishes gradually, by the second-order phase transition. This phase boundary is a complicated function of R and κ, different from the simple boundary $\kappa = 1/\sqrt{2}$, which divides the first- and second-order phase transitions in infinite (open) superconductors.[10] We consider the phase diagrams for the bounded system, found below [see Figs. 1(a), 3(a), and 5], as the main new result of the present investigation. (Similar phase diagrams exist also in thin-disk geometry, see Fig. 21 in Ref. 4c).

Other topics are touched only in passing (such as metastability, the paramagnetic Meissner effect, the pinning of vortices to the sample boundary, etc.). Such questions were studied in more detals in Refs. 2,3,6–8 (for long cylinders), and in Refs. 4,5,9 (for thin disks).

In Sec. II the mathematical side of the problem is formulated and the basic GL equations, used in calculations, are written. Sec. III contains the numerical results, alongside with necessary comments. In Sec. IV the results are summarized and discussed.

II. EQUATIONS

In what follows below, the case is considered of a long superconducting cylinder of radius R, in the external mag-
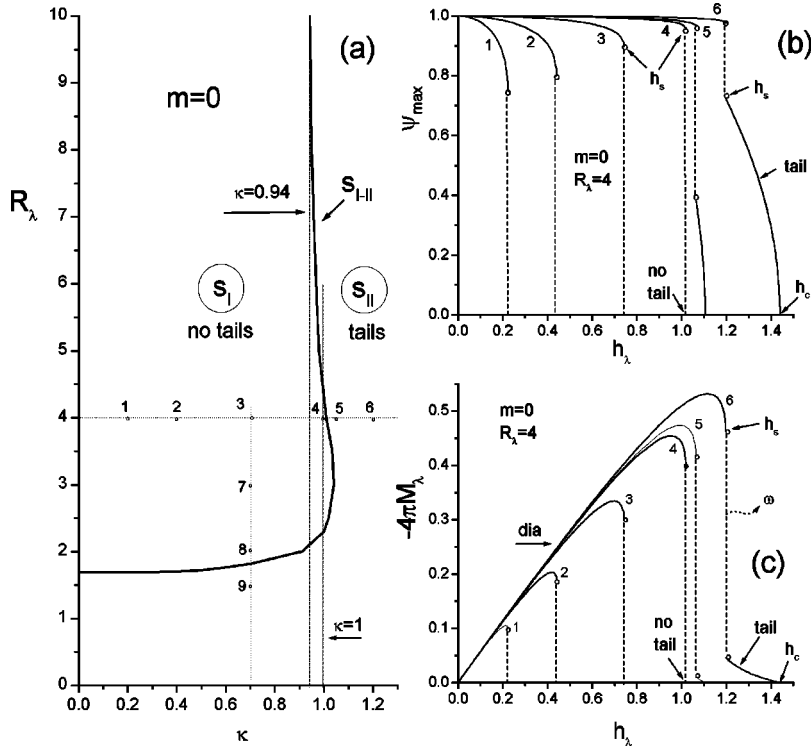
FIG. 1. (a) The boundary ($S_{\text{I-II}}$) between regions (s_{I} and s_{II}), where the first- or second-order phase transitions to normal state ($\psi \equiv 0$) in magnetic field exist. (b) The behavior $\psi_{\max}(h_\lambda)$ at the points 1–6 ($m=0$, $R_\lambda \equiv R/\lambda = 4$) in (a). In the region s_{I} the order parameter vanishes by the first-order jump. In the region s_{II} the order parameter $\psi_{\max}(h_\lambda)$ has a ''tail,'' and vanishes smoothly, by the second-order phase transition. (c) Analogous behavior for magnetization $M_\lambda(h_\lambda)$. (The possibility of the acoustic radiation during the solution transition from one branch to another is marked by the letter ω.) The peep-holes 1–9 in (a) are pierced in the points $1: \kappa=0.2$, $2: \kappa=0.4$, $3: \kappa=0.7$, $4: \kappa=1$, $5: \kappa=1.05$, $6: \kappa=1.2$ ($R_\lambda=4$), $7: R_\lambda=3$, $8: R_\lambda=2$, $9: R_\lambda=1.5$ ($\kappa=0.7$).

netic field $H \geq 0$, which is parallel to the cylinder element. In cylindrical coordinates the system of GL equations may be written in dimensionless form[7]

$$\frac{d^2 U}{d\rho^2} - \frac{1}{\rho} \frac{dU}{d\rho} - \psi^2 U = 0, \tag{1}$$

$$\frac{d^2 \psi}{d\rho^2} + \frac{1}{\rho} \frac{d\psi}{d\rho} + \kappa^2 (\psi - \psi^3) - \frac{U^2}{\rho^2} \psi = 0. \tag{2}$$

Here $U(\rho)$ is the dimensionless field potential, $b(\rho)$ is the dimensionless magnetic field, $\psi(\rho)$ is the normalized order parameter, $\rho = r/\lambda$, λ is the field penetration length, $\lambda = \kappa \xi$, where ξ is the coherence length, and κ is the GL parameter. The dimensioned potential A, field B, and current j_s are related to the corresponding dimensionless quantities by the formulas:

$$A = \frac{\phi_0}{2\pi\lambda} \frac{U+m}{\rho}, \quad B = \frac{\phi_0}{2\pi\lambda^2} b, \quad b = \frac{1}{\rho} \frac{dU}{d\rho},$$

$$j(\rho) = j_s / \frac{c\phi_0}{8\pi^2\lambda^3} = -\psi^2 \frac{U}{\rho}, \quad \rho = \frac{r}{\lambda}. \tag{3}$$

[The field B in Eq. (3) is normalized by $H_\lambda = \phi_0/(2\pi\lambda^2)$, with $b = B/H_\lambda$; instead of H_λ one can normalize by $H_\xi = \phi_0/(2\pi\xi^2)$, or by $H_\kappa = \phi_0/(2\pi\xi\lambda) = H_\xi/\kappa$. The coefficients in Eqs. (1), (2) would change accordingly.] The vorticity m in Eq. (3) specifies how many flux quanta are associated with the vortex, centered at the cylinder axis (the so-called giant-vortex state).

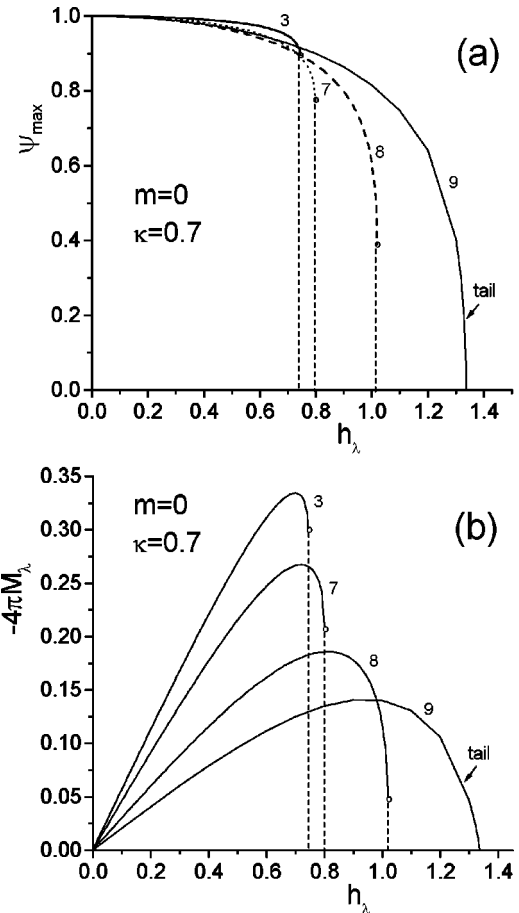The boundary conditions to Eq. (1) are

FIG. 2. The dependences (a) $\psi_{\max}(h_\lambda)$ and (b) $M_\lambda(h_\lambda)$ for $m=0$, $\kappa=0.7$. The numeration of curves corresponds to the points 3, 7–9 in Fig. 1(a).
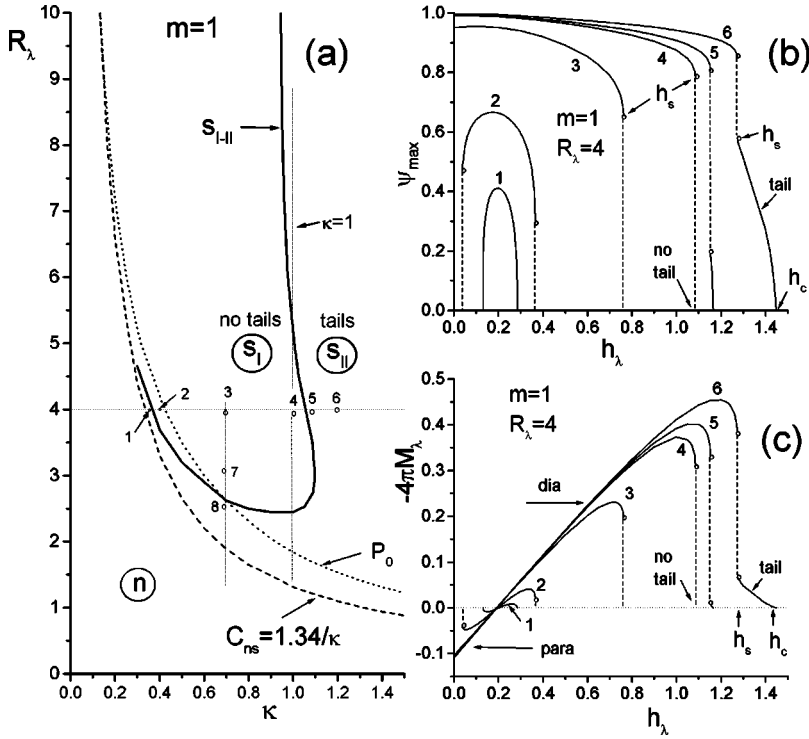
FIG. 3. Analogous to Fig. 1, but for $m=1$. The dashed curve C_{ns} in (a) separates the normal (n) and superconducting (s) regions. The curve P_0 marks the points (R_λ,κ), where the metastable vortex state ($m=1$) may still exist in absence of the field ($h_\lambda=0$) due to the pinning to the boundary. Below the curve P_0 the vortex state may exist only in presence of finite external field [$h_\lambda>0$, see the curves 1,2 in (b), (c)]. (This is an example of the field stimulation effect, or reentrant superconductivity.) The peep-holes 1–8 in (a) are pierced in the points $1:\kappa=0.35$, $2:\kappa=0.4$, $3:\kappa=0.7$, $4:\kappa=1$, $5:\kappa=1.07$, $6:\kappa=1.2$ ($R_\lambda=4$) $7:R_\lambda=3$, $8:R_\lambda=2.4$ ($\kappa=0.7$).

$$U\Big|_{\rho=0}=-m,\qquad \frac{dU}{d\rho}\Big|_{\rho=R_\lambda}=h_\lambda, \qquad (4)$$

where $R_\lambda=R/\lambda$, $h_\lambda=H/H_\lambda$. The boundary conditions to Eq. (2) are

$$\frac{d\psi}{d\rho}\Big|_{\rho=0}=0,\qquad \frac{d\psi}{d\rho}\Big|_{\rho=R_\lambda}=0\quad(m=0), \qquad (5)$$

$$\psi\Big|_{\rho=0}=0,\qquad \frac{d\psi}{d\rho}\Big|_{\rho=R_\lambda}=0\quad(m>0).$$

[The solutions, found from Eqs. (1)–(5), describe the radially symmetric giant-vortex states of fixed vorticity m. The more complicated asymmetric multivortex solutions of the same total vorticity $m=\Sigma_i m_i$ (m_i is the vorticity of a vortex, situated at arbitrary point r_i on the cylinder cross section) may be studied numerically by the methods, developed in Refs. 4,5.]

The magnetic moment (or, magnetization) of the cylinder, related to the unity volume, may be written in the form

$$\frac{M}{V}=\frac{1}{V}\int\frac{B-H}{4\pi}dv=\frac{B_{av}-H}{4\pi},$$

$$B_{av}=\frac{1}{V}\int B(\mathbf{r})dv=\frac{1}{S}\Phi_R,$$

where B_{av} is the mean field value inside the superconductor, Φ_R is the total magnetic flux, confined in the cylinder. In the normalization (3), denoting $\bar{b}=B_{av}/H_\lambda$, $h_\lambda=H/H_\lambda$, $M_\lambda=M/H_\lambda$, one finds
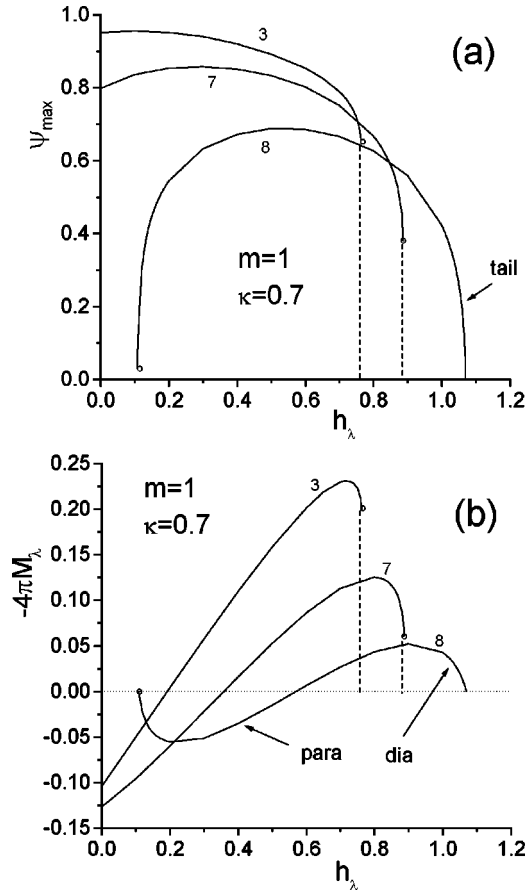

FIG. 4. Analogous to Fig. 2, but for $m=1$. The presence of paramagnetic ($M_\lambda>0$) and diamagnetic ($M_\lambda<0$) parts of magnetization is evident from (b). The numeration of curves corresponds to the peep-holes in Fig. 3(a).
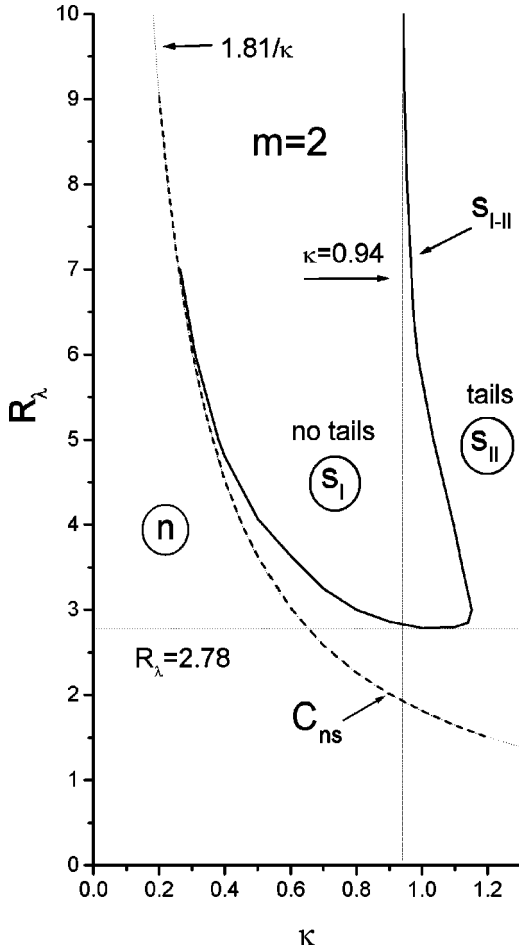
FIG. 5. Analogous to Figs. 1(a) and 3(a), but for $m=2$. The vertical asymptote $\kappa=0.94$ is the same for $m=0,1,2$. This is natural, because for large radii ($R_\lambda \gg 1$) the influence of the vortex field is negligible. The bottom part of the curve $S_{\text{I-II}}$ lays at $R_\lambda=2.78$ (with $R_\lambda=2.45$ for $m=1$, and $R_\lambda=1.69$ for $m=0$). The dashed curve C_{ns} is well approximated by the dependence $C_{ns}\approx1.81/\kappa$ (the dotted line).

$$4\pi M_\lambda=\bar{b}-h_\lambda, \quad \bar{b}=\frac{2}{R_\lambda^2}(U_\lambda+m), \tag{6}$$

$$\phi_R=\frac{\Phi_R}{\phi_0}=U_\lambda+m, \quad U_\lambda=U(R_\lambda), \quad R_\lambda=\frac{R}{\lambda}.$$

Accordingly, the normalized Gibbs free energy of the system may be written as[7]

$$\Delta g=\Delta G/\left(\frac{H_{cm}^2}{8\pi}V\right)=g_0-\frac{8\pi M_\lambda}{\kappa^2}h_\lambda+\frac{4m}{\kappa^2}\frac{b(0)-h_\lambda}{R_\lambda^2}, \tag{7}$$

$$g_0=\frac{2}{R_\lambda^2}\int_0^{R_\lambda}\rho d\rho\left[\psi^4-2\psi^2+\frac{1}{\kappa^2}\left(\frac{d\psi}{d\rho}\right)^2\right].$$

Here $\Delta G=G_s-G_n$ is the difference of free energies in superconducting and normal states, $b(0)=B(0)/H_\lambda$, $B(0)$ is the magnetic field at the cylinder axis, H_{cm}

$=\phi_0/(2\pi\sqrt{2}\lambda\xi)$ is thermodynamical critical field of massive superconductor, g_0 and is the condensation energy with account for the order parameter gradient. The expressions (6), (7) may be used for calculating the corresponding quantities.

III. NUMERICAL RESULTS

The solutions of Eqs. (1)–(5) depend on the space coordinate ρ and several parameters, for instance, $\psi(\rho)=\psi(m,R_\lambda,\kappa,h_\lambda;\rho)$ [analogously for the potential $U(\rho)$ and the field $b(\rho)$]. Let the vorticity m be fixed ($m=0,1,2,\dots$) and consider at first the case $m=0$ (the vortex-free Meissner state). Consider the plane of parameters (R_λ,κ) [see Fig. 1(a)]. In every point of this plane there exists a set of solutions of Eqs. (1)–(5), which depend parametrically on the external field h_λ. (Several points, laying along the line $R_\lambda=4$ are numerated as 1–6.) One may imagine a peep-hole, pierced in arbitrary point (R_λ,κ), which allows us to see the solutions behavior versus H. The set of solutions $\psi(h_\lambda;\rho)$ is unique for each peep-hole and may be characterized, for instance, by the field dependence of the maximal value of the order parameter $\psi_{max}(h_\lambda)$, or by the form of the magnetization curve $M_\lambda(h_\lambda)$ (6). The examples of such dependences in different points of the plane (R_λ,κ) are given in Figs. 1(b), 1(c) (only the case $h_\lambda\geq0$ is considered; some illustrations for the case $h_\lambda<0$, as well as the corresponding coordinate dependences, may be found in Refs. 2,6,7).

It is clear from Fig. 1(b), that the characteristic behavior $\psi_{max}(h_\lambda)$ depends substantially on the value of κ. For small κ, the value $\psi_{max}(h_\lambda)$ terminates by jump (the curves 1–4) at some point $h_\lambda=h_s$, where the first-order phase transition to normal state [$\psi(\rho)\equiv0$] occurs (if h_λ increases). The region, where the superconducting solutions terminate by the first-order phase transition, is marked in Fig. 1(a) as s_I.

For larger κ (the curves 5, 6) there is also a jump in $\psi_{max}(h_\lambda)$ at some point $h_\lambda=h_s$, but with a "tail" remaining on the curve. If the field h_λ increases, the superconducting solutions 5,6 vanish gradually at the point h_c, by the second-order phase transition to normal state. The region, where the superconducting solutions terminate by the second-order phase transition, is marked in Fig. 1(a) as s_{II}. [The appearance of the tail on the magnetization curve means the transition of the solution to the edge-suppressed form (see Ref. 7 for details). At the transition points (see the dashed vertical lines in Figs. 1, 2) the shape of the solutions changes, i.e., the order parameter becomes time dependent (the increment at these points becomes positive). Various nonequilibrium effects may accompany this evolution process (we mention, for instance, the possibility of electromagnetic and acoustic waves generation.[11])]

It is evident, that for small radius cylinder ($R_\lambda<1.69$) the superconducting solution terminates by the second-order phase transition, even in type-1 (i.e., small κ) superconductors.[12] The transformation of the solutions with diminishing radius R_λ is illustrated in Fig. 2 for $\kappa=0.7$.

Note, that if the line $\kappa=1$ in Fig. 1(a) is followed from large to small R_λ, the superconducting states, which exist along this line, display at first the second-order phase transi-

tion in magnetic field (for larger radii R_λ), then the first order (for intermediate R_λ), and again the second order (for smaller radii R_λ). Only, if $\kappa > 1.05$, all the solutions display the second-order behavior. Notice also, that the state $m = 0$ is totally diamagnetic ($-4\pi M_\lambda > 0$).

Because in every point of s_{II}-region the order parameter vanishes by the second-order phase transition [$\psi_{max} \to 0$, see Fig. 1(b)], the superconducting phase boundary in magnetic field, h_c, may be found analytically, by linearizing the system (1), (2) (with account, that $\psi \ll 1$ and $b \approx h_\lambda$), and passing to single linear equation for the order parameter,[13] whose solution may be expressed in terms of the Kummer functions (see also Refs. 3–5,14). However, inside the s_I region (where the solution terminates by jump from a finite value ψ_{max} to zero) the phase boundary h_s (i.e., the highest field h_λ, still compatible with the superconductivity) cannot be found by solving the linearized equation, but full system of Eqs. (1)–(5) is needed.

The analogous investigation can be carried out in the case $m = 1$ (see Fig. 3), with a single vortex on the cylinder axis. In Fig. 3(a) are shown the region s_I, where the superconducting state terminates (if the field increases) by the first-order jump to the normal state, having finite value ψ_{max} at the transition point; the region s_{II}, where the superconductivity vanishes by the second-order phase transition; and the curve S_{I-II}, which represents the boundary between the first and second-order phase transitions.

The behavior of the order parameter $\psi_{max}(h_\lambda)$ and of the magnetization $M_\lambda(h_\lambda)$ in different points of the plane (R_λ, κ) are shown in Figs. 3(b), 3(c) (and in Fig. 4). For small κ (the curves 1,2) the solutions terminate by the first-order jump. When the line S_{I-II} is crossed, the tail appears on the curves 3,4, which widens, if R_λ and κ increase. If R_λ diminishes (Fig. 4), the magnitude of the jump in ψ_{max} also diminishes, and the solutions terminate (if the field increases) by the second-order phase transition to normal state.

On the curve C_{ns} [Fig. 3(a)] the value $\psi_{max} = 0$. The letter n denotes the normal metal region ($\psi \equiv 0$); here the superconducting state ($m = 1$) is impossible. [In this region the radius R_λ is too small, and the vortex own field is too strong to be confined within the mesoscopic sample.] It is evident, that when the radius R_λ diminishes (but κ is fixed) the transition from s to n state always is the second-order phase transition, however the width of the region between the curves S_{I-II} and C_{ns} (where the second-order transitions exist) is very small for small κ. The curve C_{ns} may be well approximated by the dependence $R_\lambda \sim a/\kappa$ (or $R_\xi = \kappa R_\lambda = a$), with $a = 1.34$.

Notice, that for any point of the s region in Fig. 3(a) the magnetization function $M_\lambda(h_\lambda)$ [Fig. 3(c)] has two sections: the paramagnetic ($M_\lambda > 0$) and diamagnetic ($M_\lambda < 0$). This is because the superconducting current has two components $j_s = j_p + j_d$. One of these currents (j_p) screens the own field of the vortex ($m = 1$) and flows around the vortex axis in a counterclockwise direction (the paramagnetic current). The second current (j_d) screens out the external field h_λ and flows near the cylinder surface in clock-wise direction (the diamagnetic current). Depending on which of these currents

prevail, the magnetization [or, equivalently, the magnetic moment $M_\lambda = (1/2c)\int[\mathbf{j}, \mathbf{r}]dv$] can change sign, as function of h_λ (see Ref. 8 for details). Recall, that in the vortex-free state ($m = 0$) there exists only diamagnetic current, i.e., $M_\lambda < 0$, see Fig. 1(c). In presence of the vortex ($m = 1$), but in absence of the external field ($h_\lambda = 0$), the screening current flows in opposite direction (the paramagnetic state $M_\lambda > 0$). Such state is metastable, because the vortex-free state posesses smaller free-energy, than the state $m = 1$.[2–8] [However, the energetically metastable (excited) state may be stable relative small distortions of its shape (when the increment of perturbations is negative).]

The curve P_0 in Fig. 3(a) corresponds to the minimal radius R_λ, when the paramagnetic vortex state ($m = 1$) can still exist inside the homogeneous cylinder in absence of the field ($h_\lambda = 0$). [The metastable vortex is held inside by the pinning to the cylinder boundary.] In those points (R_λ, κ), which lay below the curve P_0, to hold the vortex inside the cylinder, it is necessary to impose a finite external field, $h_\lambda > 0$. (This corresponds to the field stimulated and reentrant superconductivity.[2–9]) Notice, that if the cylinder radius R and the parameter κ are fixed, to cross the paramagnetic pinning boundary (P_0) it is sufficient to vary only the sample temperature, because $R_\lambda = R/\lambda(T)$ (see Ref. 8 for details).

The presence of a smooth tail in the function $\psi_{max}(h_\lambda)$ [see Figs. 3(b) and 4(a) for $m = 1$] allows one (as in the case $m = 0$) to use the linear approximation ($\psi \ll 1$) for finding the upper bound of the superconducting state h_c. In the region of the first-order jumps [s_I in Fig. 3(a)], where the function $\psi(\rho)$ is not small, the linear approach fails and more rigorous analysis, based on full system of nonlinear equations (1)–(5), is necessary. [The boundaries $S_{I-II}(\kappa)$ and $C_{ns}(\kappa)$ themselves cannot be found from the linear equation, because the latter does not depend on κ.[13] The detailed comparison of the results of the rigorous and linear analysis will be reported elsewhere.]

Similarly, one can consider the higher giant-vortex states with $m > 1$ (see Fig. 5 for $m = 2$). There also exist the boundaries of the first- and second-order phase transitions, the jumps on the magnetization curves, the paramagnetic and diamagnetic currents, and other peculiarities, analogous to those, presented in Figs. 1–4.

IV. CONCLUSIONS AND DISCUSSION

Based on self-consistent solution of nonlinear system of GL equations, the boundary, S_{I-II}, is found, which separates the regions, where the superconducting giant-vortex state of a cylinder is destroyed by the external magnetic field either by the first-order jump (the region s_I), or gradually, by the second-order phase transition (the region s_{II}). This boundary is a complicated function of the parameters (m, R_λ, κ) [see Figs. 1(a), 3(a), 5]. Note, that in the case of an infinite (open) superconductor the phase boundary between the first- and second-order transitions lays at the value $\kappa = 1/\sqrt{2}$.[10] [At this value the surface energy σ at the interface of superconducting and normal metals vanishes, and the magnetization $M(H)$ acquires a smooth tail.[10]] However, the case of infi-

nite superconductor is degenerated, in the sense that the total number of vortices in the open system cannot be defined. Due to this degeneracy there are many solutions of the system (1), (2) with different m, and it is possible to consider the superconducting state as a linear combination of states with different vorticities.[10] In the bounded system this degeneracy is removed, and it is necessary to consider the states of fixed total vorticity $m = \Sigma_i m_i$ (the quantum number m is now a topological invariant, so it is not permissible to consider the mixture of states with different m). [Notice, that the linear combination of different states, considered by Yampolsky and Peeters,[4f] Eq. (22), satisfies the conservation condition $m = \Sigma_i m_i = \text{const}$; instead of m and m_i they use the quantum-mechanical angular momenta notations, L and L_i (see also Refs. 3,5).]

The mentioned difference of the $S_{\text{I-II}}$ boundary from the value $\kappa = 1/\sqrt{2}$ is due to the difference in geometries and to the account of the space-quantization effects, present in the bounded system. (To trace the limiting transition from the bounded to open geometry, it might be necessary to consider the case of flattened elliptical cylinder, which models better the geometry of infinite slab, adopted in Ref. 10.)

We mention in conclusion that the main attention in the present work was drawn to the mathematical side of the problem: to find the $S_{\text{I-II}}$ boundary for the giant-vortex state of fixed vorticity m. It is clear, that such state may decay into the multi-vortex configuration of the same vorticity, $m = \Sigma_i m_i$, and to find the most stable (equilibrium) vortex configuration it would be necessary to compare the Gibbs free energies of the corresponding states. To find self-consistent solution in a case of a general multivortex configuration is a very difficult task, which was not handled in the present paper. (The examples of such solutions for thin-disk geometry with various boundary conditions may be found in Refs. 4,5,9) Some of the edge-suppressed giant-vortex states might be metastable (having larger free-energy than the equilibrium configuration). However, as is well known, the physical system not necessarily must be in equilibrium, but may remain in the excited metastable state. Such metastable states manifest themselves in the hysteresis, superheating and supercooling phenomena, in the paramagnetic Meissner effect, in the jumps of magnetization, and in others peculiarities of the mesoscopic samples behavior, observed experimentally.[9] For this reason, the one-dimensional giant-vortex states are interesting not only as an example of self-consistent solutions of one-dimensional nonlinear equations, but, may possibly be used in the interpretation of some experimental details. Thus, further analysis of the questions, raised in the present paper (as well as the possible connection with experiment), is necessary.

[1] V.L. Ginzburg and L.D. Landau, Zh. Eksp. Teor. Fiz. **10**, 1064 (1950).

[2] H.J. Fink *et al.*, (a) Phys. Rev. **151**, 219 (1966); (b) **168**, 399 (1968); (c) Phys. Rev. B **20**, 1947 (1979).

[3] V.V. Moshchalkov, X.G. Qiu, and V. Bruyndoncx, Phys. Rev. B **55**, 11 793 (1997).

[4] V. Schweigert *et al.*, (a) Phys. Rev. Lett. **79**, 4653 (1997); (b) Superlattices Microstruct. **25**, 1195 (1999); (c) Phys. Rev. B **57**, 13 817 (1998); (d) **59**, 6039 (1999); (e) Physica C **332**, 266 (2000); **332**, 426 (2000); **332**, 255 (2000); (f) S. Yampolsky and F. Peeters, Phys. Rev. B **62**, 9663 (2000).

[5] J.J. Palacios, Phys. Rev. B **58**, R5948 (1998); Physica B **256-258**, 610 (1998); Phys. Rev. Lett. **83**, 2409 (1999); **84**, 1796 (2000).

[6] G.F. Zharkov and V.G. Zharkov, Phys. Scr. **57**, 664 (1998); G.F. Zharkov, V.G. Zharkov, and A.Yu. Zvetkov, Phys. Rev. B **61**, 12 293 (2000).

[7] G.F. Zharkov, V.G. Zharkov, and A.Yu. Zvetkov, cond-mat/0008217 (unpublished).

[8] G.F. Zharkov, Phys. Rev. B **63**, 214502 (2001).

[9] W. Braunish *et al.*, Phys. Rev. B **48**, 4030 (1993); L. Pust *et al.*, *ibid.* **58**, 14 191 (1998); A.K. Geim *et al.*, Nature (London) **373**, 319 (1995); **390**, 259 (1997); **407**, 55 (2000); L. Chibotaru *et al.*, *ibid.* **408**, 833 (2000); B. Muller-Alinger and A.C. Motta, Phys. Rev. Lett. **84**, 3161 (2000).

[10] A.A. Abrikosov, *Fundamentals of the Theory of Metals* (North-Holland, Amsterdam, 1988).

[11] A.M. Gulian and G.F. Zharkov, *Nonequilibrium Electrons and Phonons in Superconductors* (Kluwer Academic/Plenum Publishers, New York, 1999).

[12] V.L. Ginzburg, Zh. Exp. Teor. Fiz. **34**, 113 (1958) [Sov. Phys. JETP **7**, 78 (1958)].

[13] D. Saint-James and P. de Gennes, Phys. Lett. **7**, 306 (1963); **15**, 13 (1965).

[14] Yu.N. Ovchinnikov, Sov. Phys. JETP **52**, 755 (1980).